

# Rotation and Twist of the Central-Pair Microtubules in the Cilia of *Paramecium*

CHARLOTTE K. OMOTO and CHING KUNG

Laboratory of Molecular Biology, University of Wisconsin, Madison, Wisconsin 53706. Dr. Omoto's present address is the Department of Biology, Princeton University, Princeton, New Jersey 08544.

**ABSTRACT** The orientation and configuration of the central-pair microtubules in cilia were studied by serial thin-section analysis of "instantaneously fixed" paramecia. Cilia were frozen in various positions in metachronal waves by such a fixation. The spatial sequence of these positions across the wave represents the temporal sequence of the positions during the active beat cycle of a cilium. Systematic shifts of central-pair orientation across the wave indicate that the central pair rotates 360° counterclockwise (viewed from outside) with each ciliary beat cycle (C. K. Omoto, 1979, Thesis, University of Wisconsin, Madison; C. K. Omoto and C. Kung, 1979, *Nature [Lond.]* 279:532-534). This is true even for paramecia with different directions of effective stroke as in forward- or backward-swimming cells. The systematic shifts of central-pair orientation cannot be seen in Ni<sup>++</sup>-paralyzed cells or sluggish mutants which do not have metachronal waves. Both serial thin-section and thick-section high-voltage electron microscopy show that whenever a twist in the central pair is seen, it is always left-handed. This twist is consistent with the hypothesis that the central pair continuously rotates counterclockwise with the rotation originating at the base of the cilium. That the rotation of the central pair is most likely with respect to the peripheral tubules as well as the cell surface is discussed. These results are incorporated into a model in which the central-pair complex is a component in the regulation of the mechanism needed for three-dimensional ciliary movement.

Cilia (eucaryotic flagella and sperm tails) have been studied to determine the function of the components responsible for generating motion (reviewed in references 4, 14, and 40). The sliding-microtubule model is now accepted as the fundamental motile mechanism for cilia. In the late 1960's Satir (39) produced the first evidence for sliding rather than contraction as the basis for ciliary motion. The sliding-microtubule hypothesis was given support by the direct demonstration of sliding disintegration in trypsin-treated axonemes by Summers and Gibbons (46). The force that causes the ciliary microtubules to slide is generated by the pair of dynein arms that project out periodically along the length of each peripheral microtubule doublet (11). Sliding was shown to be unipolar by Sale and Satir (37) in *Tetrahymena* cilia.

Studies indicate some interaction between the radial spokes of the peripheral doublets and the projections from the central pair (47, 51). It is suggested that such an interaction converts sliding to bending, but how sliding of the peripheral doublets is transduced into active coordinated beating of cilia is not known. The functions in motility of such components as the radial spokes and the central-tubule complex are largely un-

known. Nevertheless, they must be essential because mutational loss of these components results in paralysis (32, 45, 52).

To create and propagate ciliary bends, the sliding of the nine doublets must be regulated. One can conceive of the regulation as involving two components: a circular coordination and a longitudinal coordination. On the circumference of the radially symmetric axoneme, the force generated by the unipolar sliding on one side is directly opposed by that of the other side. Thus, the sliding must be regulated to allow one side of the cilium (e.g., only one peripheral doublet) to slide actively while the others slide passively. Longitudinally, sliding must also be regulated, for if there were uniform sliding along the whole length of a cilium, one would see only that sliding, not the observed bending. To obtain a bend from sliding, one might imagine a length of the cilium where sliding is inhibited, another segment where active sliding takes place (perhaps the region of the bend), and yet another segment where the resultant sliding is passively conducted to the tip (41). Because the central-pair microtubules form an asymmetric structure in the radially symmetric axoneme and run the full length of the cilium, they may well play a regulatory role. The bending

motion of the cilium can be analyzed in terms of the forces generated by the sliding, and many aspects of ciliary motion have been simulated by computer models using these forces (for example, see references 3 and 26). However, concrete mechanisms for the orderly activation of these forces remain obscure. We describe here a different approach in which attention is focused on the central-pair microtubules as a possible regulatory structure. We examine the configuration and those movements of the central pair that may be related to the beat cycle. Change in the orientation of the central pair was first noted by Satir (39) and Tamm and Horridge (49).

To study possible changes in the orientation of the central-pair microtubules, we have taken advantage of the naturally occurring metachrony of the cilia on the paramecium surface. While each cilium goes through its own beat cycle, consisting of a rapid effective stroke (phase 5 directly to phase 1, Fig. 1A), neighboring cilia along a certain direction are slightly out of phase. The systematic phase lag leads to the metachronal waves and their propagation on the paramecium surface. At any instant, the cilia along the direction of wave propagation are in successively earlier phases of their own beat cycle (Fig. 1B, from left to right). Perpendicular to this direction and parallel to the wave front, one finds cilia at the same phase of beat forming lines of synchrony. These lines parallel the direction of the effective stroke. Our strategy has been to fix the paramecium surface instantaneously and thereby retain the spatial sequence of cilia in the frozen waves. Once the paramecium surface is "instantaneously fixed," we can then perform electron microscope analysis of the ultrastructures, especially of the orientation of the central-pair microtubules. Similarity of this orientation along lines of synchrony and a gradual and systematic change of this orientation in the direction of

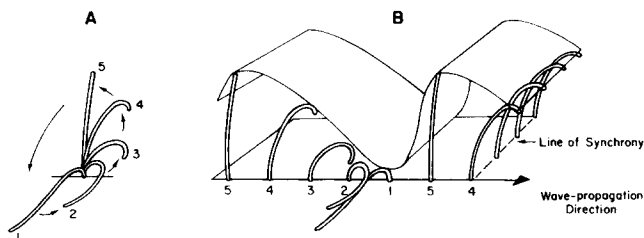


FIGURE 1 The temporal and spatial sequence of *Paramecium* cilia. (A) The temporal sequence of a beating cilium. From phase 1, 2, 3, 4, to 5 is the three-dimensional recovery stroke. From phase 5 to phase 1 is the planar effective stroke that powers the paramecium's locomotion. This cycle repeats incessantly at  $\sim 20$  Hz in normal situations. Viewed from above, the tip of the cilium traces a semi-circle counterclockwise. (B) The spatial sequence of cilia on the paramecium surface. Along any one line of synchrony, all cilia are at the same phase of beat. One such line at phase 4 is shown. Along the perpendicular to the lines of synchrony, neighboring cilia show a phase shift which results in the metachronal waves on the surface. Because in the next moment, the cilium labeled 5 will be in phase 1, cilium 1 will be in phase 2, cilium 2 in phase 3, etc., the waves propagate toward the right in this diagram. Opposite this direction (from right to left), we find cilia in sequentially later phases of the beat cycle (i.e., phase 1, 2, 3, 4, 5, 1), corresponding to the temporal sequence shown in A. These waves can be preserved by instantaneous fixation whereby the cilia are frozen in a spatial sequence that relates to the temporal sequence and is ready for ultrastructural analyses. The forms of the ciliary beat and the waves are similar in paramecia swimming forward or backward, although the effective strokes and, therefore, the lines of synchrony differ by  $120^\circ$ – $150^\circ$  in the two cases.

wave propagation is correlated to the beat cycle. The method of instantaneous fixation of ciliated protozoa was first worked out by Parducz (31) for light microscope work and later modified by Tamm (personal communication) for electron microscope studies. Tamm and Horridge (49) used this approach to study the orientation of the central-pair microtubules in *Opalina*. They and other previous workers did not distinguish the two members of the central pair. Therefore, although movement of the central pair during the ciliary beat can be shown, complete rotation of the central pair, if it exists, cannot be demonstrated. The two members of the central pair of *Paramecium* cilia can be distinguished by ultrastructural markers (7, 29, 30). A vector from the tubule without the marker to the one with the markers can therefore be drawn unambiguously and its angular changes determined. Furthermore, methods of ionic and genetic manipulations of *Paramecium* behavior are well established (8, 28). We can therefore investigate this vector and its possible rotation in backward-swimming cells or immobilized cells as well as in the normal forward-swimming cells.

## MATERIALS AND METHODS

### Culture Conditions

*Paramecium tetraurelia* (formerly syngen 4 of *P. aurelia*, Sonneborn (43)) were cultured at  $28^\circ\text{C}$  in phosphate-buffered 10% Cerophyl medium (Cerophyl Laboratories, Kansas City, Mo.) which had been inoculated with *Enterobacter aerogenes* and incubated at  $30^\circ\text{C}$  for at least 20 h before use (42). Wild-type stock 51s, non-kappa bearing, and a sluggish mutant, d4-600 derived from 51s were used (23).

### Fixation

Instantaneous fixation, based on osmium tetroxide (31, 47) modified for transmission electron microscopy of *Paramecium* (Tamm, personal communication) was used.

The paramecia were filtered through six layers of cheesecloth to remove debris and washed either in Tris-Ca solution (1 mM  $\text{CaCl}_2$ , 1 mM Tris-HCl, pH 7.2) or in Dryl's solution (6) (1 mM  $\text{NaH}_2\text{PO}_4$ , 2 mM  $\text{Na}_3$  citrate, 1.5 mM  $\text{CaCl}_2$ ). The cells in a depression plate under the dissecting microscope were made to swim vigorously in the desired direction or were immobilized. To obtain forward-swimming cells, 4 mM  $\text{CaCl}_2$ , and 1 mM Tris-HCl, pH 7.2 (22) were pipetted onto a small drop of cells concentrated in the wash solution. For backward-swimming cells, 20 mM KCl, 0.3 mM  $\text{CaCl}_2$ , and 1 mM Tris-HCl, pH 7.2 were used instead. To immobilize cells, 10 mM  $\text{NiCl}_2$  was added to the solution for forward swimming. This solution immobilized cells within 10 s. All chemicals were of reagent grade.

The cells were then fixed by quickly pipetting a solution of 2% glutaraldehyde (EM grade), 2%  $\text{OsO}_4$ , 50 mM Na-K phosphate, pH 7.2. This solution must be freshly made, because the  $\text{OsO}_4$  reacts with glutaraldehyde, and becomes ineffective for fixation. At least four times the volume of fixative was added to the paramecium solution and allowed to fix for 10–15 min. The rapid action of the fixative apparently freezes the cilia because the metachronal waves preserved by this method are like those deduced from high-speed cinematography of live cilia (24).

### Transmission Electron Microscopy

The fixed cells were washed with distilled water, postfixed in 0.5% uranyl acetate, dehydrated through an ethanol series, and then flat-embedded in either Epon-araldite (27) or Spurr's resin (44). Individual embedded cells were examined for the presence of metachronal waves with Nomarski optics, cut out, mounted in a known orientation onto a plastic peg, and sectioned on a Reichert OmU2 ultramicrotome. Serial sections were taken near the cell surface  $\sim 2\ \mu\text{m}$  into the cell (25–35 sections). Ribbons of serial sections were picked up on Formvar-coated loops and transferred to single-slotted grids. The sections were stained at room temperature either with 7.5% uranyl magnesium acetate (10) for 2 h followed by 5 min in Reynolds' lead citrate (34) or 1% potassium permanganate (2) for 2 min followed by 5 min in Reynolds' lead citrate. Sections were examined and photographed on a Philips 300 or a JEM-100S electron microscope.

## Analysis of the Central-Pair Orientation from Instantaneously Fixed *Paramecia*

We analyzed the orientation of the central pair in the 300-nm proximal region of the cilia just above the basal body. We restricted our analysis to this area, because, unlike the distal shaft of the cilium, this region being closed to the basal body, is perpendicular to the section plane, and central-tubule insertion into the axosome can be scored in this region. This proximal region gives clear cross sections of the cilia necessary for determining the central-pair orientation. The orientation of the central pair is unambiguously determined because the two members can be distinguished. Two independent markers available on *Paramecium* cilia are: the 10-nm central-tubule spur and the central-tubule insertion into the axosome (Fig. 2). It has been determined by serial-section analysis that both markers identify the same central tubule (29, 30). A central-pair vector, drawn from the tubule without the markers to the one with, can only be accurately measured for those cilia in which the central pair is approximately perpendicular to the section plane. Thus, only the mid-portion of the paramecium surface on one or two sides of the cell is analyzed. Up to five metachronal waves can be seen in this region.

Photographs were taken at magnification low enough to minimize the number of composite photographs necessary to show the entire surface examined, but high enough to score for central-tubule markers (approx.  $\times 3,000$ ). Negatives were further magnified 3.5 times on an enlarger and prints were made. The prints were then organized into a sequence of serial sections. Whenever necessary, prints were cut and taped to make composites of larger cell surfaces. Visual inspection of these micrographs already suggests systematic changes in the orientation of the central-pair microtubules, as shown in Fig. 2. For more formal analysis, the outline of the section, all cilia unit territories and other features useful for later

alignment of the serial sections were traced. The central-pair markers (either the spur or the insertion into the axosome, or both) were noted. The tracings of consecutive serial sections were superimposed. Each cilium was numbered on each of the tracings of serial sections and the numbering was maintained throughout the series.

Because we do not analyze the full length of the cilia on the paramecium but concentrate only on the transition region near the body surface, we do not reconstruct a three-dimensional view of the cilia, as diagrammed in Fig. 1*B* where the direction of the wave and the line of synchrony are obvious. These coordinates must be reconstructed on the limited sections available. Because the paramecium surface is curved, a section that cuts certain cilia at the transition region where we perform our analyses of the central pairs also cuts other cilia at a more distal level. These more distal sections are very useful in estimating the line of synchrony because they slice various cilia at different angles. The erect cilia at the crest of the metachronal waves are cut in cross sections; the segments of the cilia which lie down near the wave trough are cut in long sections or are missing from the slice; cilia between these two extremes are in tangential sections. Thus, cilia that are cut to give the same section images are of the same posture. The line through these cilia is therefore a line of synchrony. The curved tangential sections and the long sections also indicate the direction of the effective stroke along this line of synchrony. Note, however, that this line cannot be drawn accurately because it involves subjective judgments on the various images. Fig. 3 is an example of a low-power electron micrograph from which the distal sections of cilia can be recognized and line *A*'s are approximated.

A line (line *A*), approximated as the lines of synchrony using images from distal sections, was drawn on all the serial sections, taking care to have the lines in all sections parallel. Using these lines, each of the central-pair vector angles determined from the proximal sections was measured using a protractor. Setting this line *A* in the direction of the effective stroke  $\pm 20^\circ$  as sector 9,  $40^\circ$  angle

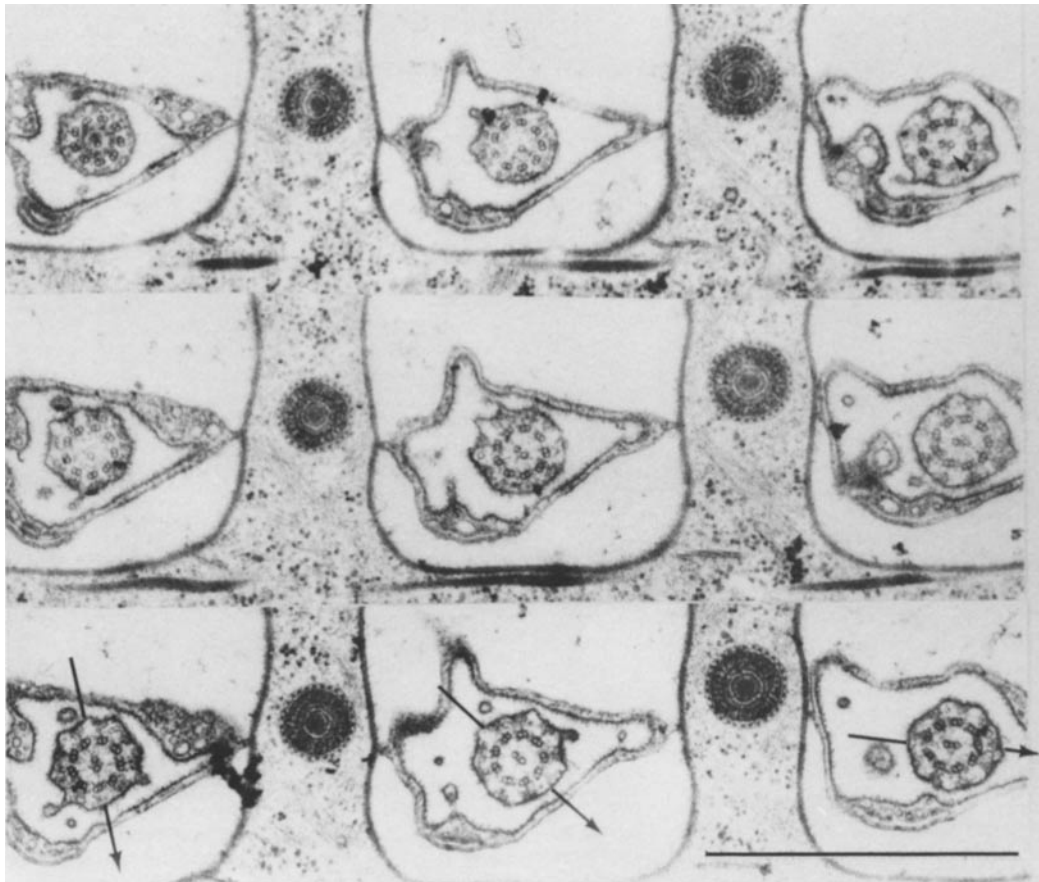


FIGURE 2 Serial sections of three adjacent cilia near the cell surface of a paramecium instantaneously fixed during backward swimming. In the most distal section, the central-pair vector is shown by arrows. Vector orientations were determined using the central-tubule insertion into the axosome in the left and middle cilia, or the central-tubule spur in the left and right cilia (see small arrow on the cilium on the right) in these three sections. Double identification can be made when more sections in the series are examined. Each cilium resides in a "unit territory" (i.e., the membrane structure, rectangular in section at this level), and between these units are the trichocysts (whose tips are the concentric circles in these sections). These and other features help us align the serial sections. The top row is the most proximal section. Anterior of the cell is to the left of the figure. The right side of the cell is to the bottom of the figure. The line of synchrony is from the upper left to the lower right of this figure. Bar,  $1 \mu\text{m}$ .  $\times 40,000$ .

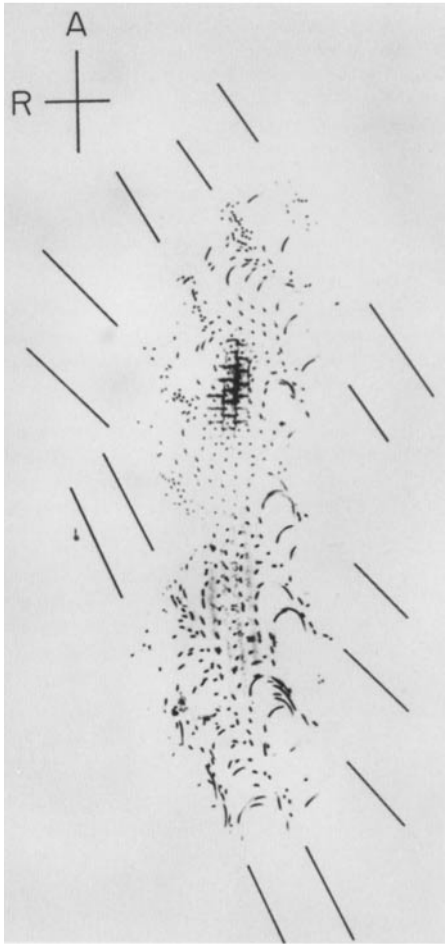


FIGURE 3 Composite low-power electron micrograph of a paramecium in thin section. A small region of the cell in glancing section is surrounded by many sections of cilia. Each of the lines drawn is meant to reflect the orientation of the corresponding cluster of near cross sections of cilia. These lines, called line A's, are thus rough estimates of the lines of synchrony at the wave crests (i.e., the effective stroke). The distances between lines are estimates of metachronal wavelength. The general cell coordinates are indicated by A (anterior) and R (cell's right).  $\times 1,400$ .

sectors were numbered clockwise (looking from the outside). The classification of the angles into nine sectors is arbitrary but reflects the imprecision in the angle measurements. The imprecision is caused by several factors. There are errors in aligning serial sections, although these errors are  $<3^\circ$  in adjacent sections. The vector drawn through the central tubules also contains an error inherent in drawing a line through the centers of two closely spaced objects, i.e., the central tubules' cross sections at the magnification used. It is estimated that this error is  $<10^\circ$ .

A simple map was drawn to facilitate analysis. All the cilia with the measured vectors of the central pairs were represented by points with Cartesian coordinates corresponding to their relative location on the cell surface. Each point was coded for its vector angle. In the cases where metachronal waves are present, (i.e., forward- or backward-swimming cells) it was noted that cilia with central pairs having similar vector angles were grouped on the map.

A best-fit set of parallel lines was drawn through groups of cilia with the central-pair vectors falling in the same sector. The grouping is subjective, but is obvious in the cases of the cells with metachronal waves. The coordinates for cilia with the same sector angles of central-pair vectors, within each of the clusters, were grouped for covariance analysis. The analysis gave the slope for the best-fit set of parallel lines (line B) through all the central tubules with the same sector angle. Line B was found to be similar to lines A in all cases with obvious metachronal waves. Because angular difference between the two lines was estimated to the  $<25^\circ$ , no attempt was made to adjust for this small angular difference. Thus line A was retained for vector measurements while the more accurate line B was used to measure distance. Any systematic distortion of the vector distribution would be less than one sector. Fig. 4 is a diagram showing the

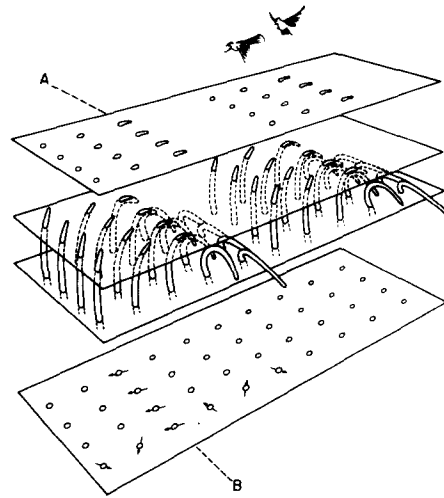


FIGURE 4 A stylized diagram showing the relation of line A, line B, and the line of synchrony. Paramecium cilia with their metachronal waves are fixed. Cilia of the same posture are on lines of synchrony. The cilia are cut by a distal (near the tips of the cilia) and a proximal (near the bases) plane as shown in the central portion of the diagram. These two planes with cilia in section views are redrawn as the upper and the lower planes in the diagram. On the upper plane, different section images appear depending on the postures of the cilia. The lines (line A's) through similar images on this plane approximate the lines of synchrony. An actual case where line A's are determined is shown in Fig. 3. On the lower plane, the central-pair orientations (arrows) found in the population of cross-sectioned cilia allow an independent grouping. Groups of cilia with similar orientations define line B's. A computerized covariance analysis of all orientations is made to best fit the lines to the data. Line B's are found to be parallel or nearly parallel to line A's in the actual studies of instantaneously fixed paramecia.

relation of the line of synchrony, line A and line B.

A line was drawn with the slope determined by computer covariance analysis (line B) at the edge of the map. The distances of cilia from line B (ordinate) were plotted against the central-pair vector angle represented by  $40^\circ$  sectors (abscissa) (Figs. 6 and 7). Neighboring cilia with the same central-pair orientation were grouped (vertical brackets). The line was drawn through cilia or groups of cilia of successively increasing distance ( $d$ ) from the line of reference (line B).

### Analysis of Possible Twist of the Central Pairs

**SERIAL, THIN CROSS SECTIONS OF INDIVIDUAL CILIA:** 6-15 serial sections of each of the cilia were analyzed. An arbitrary line of reference, fixed with respect to features such as the outline of the section, cilia and unit territories, is drawn through all the sections. The angle between the line through the centers of two tubules and the line of reference is measured for each ciliary cross section on each of the serial sections.

**THICK-SECTION HIGH-VOLTAGE ELECTRON MICROSCOPE STUDIES OF CILIARY CROSS SECTIONS:** 0.25- to 0.5- $\mu\text{m}$  sections were cut from material embedded in Epon-araldite, stained in a humidior at  $50^\circ$ - $60^\circ\text{C}$  by complete immersion in 7.5% uranyl magnesium acetate for 4-20 h, washed, and then stained by completely immersing in Reynolds' lead citrate for 30-60 min at room temperature. The sections were then carbon coated and viewed at 800-1,000 kV on the AEI EM 7 million-volt High Voltage Electron Microscope (HVEM), NIH Biotechnology Resource at the University of Wisconsin. Segments of cilia are photographed at two different angles on the goniometer stage with tilt angles from  $<20^\circ$  to  $>80^\circ$ . The two images produced are studied as "tilt pairs" or "in stereo" to determine the handedness of the twist. The proper viewing of the stereo or tilt pairs to obtain the absolute handedness of the samples were determined (by Dr. H. Ris) using independent specimen with known orientation.

**LONGITUDINAL THIN SECTION:** Thin sections which parallel the long axis of a cilium for  $1\ \mu\text{m}$  or more show the central tubules in various configurations (Fig. 5). Thickness of thin sections ranges from 70 to 90 nm. The thickness is adequate to include both central tubules in the section while not including any superimposing peripheral tubules to confuse image interpretation. In a longitu-

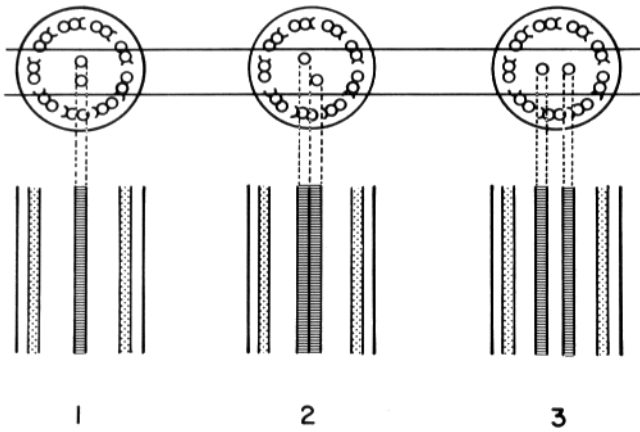


FIGURE 5 Diagram to show three different configurations of the central pairs seen in longitudinal section. Top row of ciliary cross sections shows the different orientations of the central tubules to the section plane drawn as the two horizontal lines. The bottom row shows the corresponding longitudinal images of the central pairs. Note that, in reality, with distinguishable members of the pair, two different orientations each are possible to give the images 1 and 3 and four positions are possible for image 2. (1) The two central tubules are stacked and the image of only one tubule in the longitudinal section is seen. (2) The overlapping images of the two central tubules. (3) The two central tubules in full view with a clear space between them in the longitudinal section. For this analysis, it is crucial that the 70- to 90-nm section passes through the center of the axoneme. That this is the case is shown by the distance between the peripheral tubules in section. Had the section gone through the axoneme off center, this distance would be  $<120$  nm. Such sections are excluded from our analysis.

dinal section there are three general types of central-pair images (labeled 1–3 in Fig. 5). When the section plane is nearly perpendicular to the plane through the two tubules, the two tubules are stacked and only one is seen (1). If the section plane is nearly parallel to the plane of the central tubules, both tubules are in full view with a clear space between them (3). At an intermediate central-pair orientation, the two tubules will be seen to overlap with no clear space between them (2). Transition from the separated (3) to the stacked position (1) in the longitudinal section of the same cilium indicates  $\sim 90^\circ$  twist.

### A Note Regarding the Directionality

Following the anatomists' convention, ciliary cross sections and cell coordinates are viewed from the organism's viewpoint. However, because movement is normally seen from outside the organism, both ciliary beat pattern and ultrastructural movements are described with the engineers' convention, i.e., as viewed from the outside.

## RESULTS

### Forward-Swimming cells

The findings on the orientation of the central pairs in paramecia fixed during forward swimming have been presented elsewhere (29, 30). These findings, in brief, are as follows:

(a) Lines of synchrony, as estimated from more distal sections (line *A*) have a slope similar to the slope of the best-fit lines drawn by the computer through the cilia with the same central-pair orientation (line *B*). The two lines differ by  $6^\circ$ – $25^\circ$  in different specimens.

(b) The vector angles measured for the central pairs are not uniform but span all nine, or eight out of the nine, possible sectors, indicating possible movement of the central pairs. The distribution of the central pairs at various sectors is uneven.

(c) The central-pair orientation shifts systematically in the

counterclockwise direction (looking from the tip) in cilia in the sequence of their beat cycle, (i.e., the cilia located along the perpendicular to the line of synchrony and in the direction opposite that of wave propagation, as explained in Materials and Methods). This shift in orientation is continuous, with the exception of a few of the cilia.

(d) The mean distance between groups of central pairs of the same orientation is similar to the metachronal wavelength estimated from more distal sections. Both are  $\sim 8 \mu\text{m}$ .

These observations are consistent with the view that the central pairs in the cilia rotate counterclockwise during ciliary beat and are frozen *in situ* at the instant of fixation. Because the shift in the central-pair orientation is continuous and the distance between groups of cilia with the same central-pair orientation approximates the metachronal wavelength, the simplest interpretation is that the central pair rotates  $360^\circ$  per beat cycle.

There is, however, the possibility that the orientation of the central pairs with respect to the cell body, as found in the forward-swimming cells, is fixed and that the static pattern is caused by some developmental process during ciliogenesis. This static pattern matches the metachronal waves of the forward-swimming cells but may have nothing to do with the ciliary beat cycle. To test this possibility, backward-swimming paramecia were studied. Backward-swimming paramecia beat their cilia and propagate metachronal waves in a different direction from that of the forward-swimming cells. If the pattern of central-pair orientation is fixed, it should not change when the ciliary beat direction is changed. On the other hand, if this pattern is not static and is related to the beat cycle, one would expect a systematic change when the beat direction is changed.

### Backward-Swimming Cells

Machemer (24) and others have shown, by cinematography and other methods, that the cilia of backward-swimming paramecia beat with their effective stroke toward the anterior left of the cell instead of posterior left as in the forward-swimming ones. While the beat form is similar, the beat direction changes  $120^\circ$ – $150^\circ$  counterclockwise when the paramecia swim backward. Because the direction of the effective stroke defines the direction of the line of synchrony, there is correspondingly a  $120^\circ$ – $150^\circ$  counterclockwise change in the line of synchrony when the paramecia swim backward.

When we examined paramecia instantaneously fixed during their backward swimming by light microscopy and by scanning electron microscopy, we found that the metachronal waves were well-preserved on the paramecium surface, as in the case of the forward-swimming cells. However, the lines of synchrony of the waves were from the cell's posterior right to anterior left in the backward-swimming cells instead of from anterior right to posterior left as in the forward-swimming cells. The angle difference between the two sets of lines is indeed  $\sim 120^\circ$ – $150^\circ$ .

The wave pattern is also revealed in the serial sections. In sections more distal from the paramecium surface, the wave pattern can be recognized from the different ways in which the cilia are cut by the section plane, depending on their postures in the frozen wave (see Material and Methods). The lines of synchrony (line *A*), indicated by cilia cut in the same manner, are found to be in the direction of the cell's posterior right to anterior left in the cells fixed during backward swimming. These lines in the direction of the effective stroke form an angle  $\sim 160^\circ \pm 10^\circ$  with the anterior to posterior axis. In the

sections of forward-swimming cells, this angle is  $\sim 30^\circ$ . Because one can no longer use the three-dimensional cell shape to define the coordinates on the sections, we used the kinetodesmal fibers as compasses. Bundles of kinetodesmal fibers emanate from the basal body of a cilium and extend to the right and then directly toward the anterior of the paramecium (21). Basal bodies and kinetodesmal fibers are seen clearly on the more proximal sections.

The cilia on the sections are mapped and their central-pair orientation is marked. Surveys of such maps show that the central-pair orientation is not uniform. The angles measured for the central pairs span all the nine possible  $40^\circ$  sectors. When best-fit lines are drawn through cilia with the same central-pair orientation according to the computerized covariance analysis, these lines (line *B*) are found to be very similar to the lines *A* in their slopes. In the case shown in Fig. 6, for example, line *A* and line *B* differ by only  $24^\circ$ .

By plotting the distance of the cilium from a line of reference (line *B*), against the central-pair orientation, we found a systematic shift of the orientation (Fig. 6). The orientation of the central pair shifts gradually in the counterclockwise direction (i.e., sector 1, 9, 8, 7, etc. in Fig. 6), as we examine cilia closer and closer to the line of reference (i.e., in the order of decreasing *d* from 30 to  $0 \mu\text{m}$  in Fig. 6). As explained in Fig. 1, this spatial order represents the temporal order of the beat cycle of actively beating cilia. The gradual shift in central-pair orientation can be directly seen in micrographs (Fig. 2). In the case shown in Fig. 4, three complete cycles of continuous shift are seen. The distance between groups of cilia with the central-pair orientation is  $7.9 \pm 1.0 \mu\text{m}$ , whereas the metachronal wavelength estimated from more distal sections is  $7\text{--}12 \mu\text{m}$ .

Thus, the general pattern of central-pair orientation relative to the line of synchrony in the backward-swimming paramecia is analogous to that of the forward-swimming ones, although the lines of synchrony have changed by  $120^\circ\text{--}150^\circ$ . These observations rule out the possibility that the systematic shifts in the central-pair orientation are caused by a predetermined static pattern.

### Cells without Metachronal Waves

To test further whether the change in central-pair orientation is correlated with the phase of the beat, we searched for a systematic change in central-pair orientation in paramecia that do not have cilia organized in metachronal waves. Cells whose cilia have been immobilized with  $\text{Ni}^{++}$  ions lose their metachronal waves. Cells immobilized in this fashion show some sporadic ciliary motion, but their cilia exhibit no coordinated beating characteristic of metachronal waves. Scanning electron micrographs of such cells show the disarray of cilia (29).

The map of such a cell shows no clear clustering of cilia with similar central-pair vector angles. Because such cells have no metachronal waves and no clearly defined line of synchrony, the standard analysis using metachronal waves cannot be performed. To obtain a line of best fit in the standard analysis, naturally clustered sets of cilia with the same central-pair vector angle are grouped for use in covariance analysis. Assigning cilia to a natural grouping for cells lacking metachronal waves is difficult and very arbitrary. A mock analysis was done by assuming a certain line of synchrony and arbitrarily dividing groups of cilia with the same central-pair vector angle. The slope given by covariance analysis has a poor fit to the data ( $R^2 = 25.3\%$  as opposed to  $55\text{--}69\%$  for those with metachronal

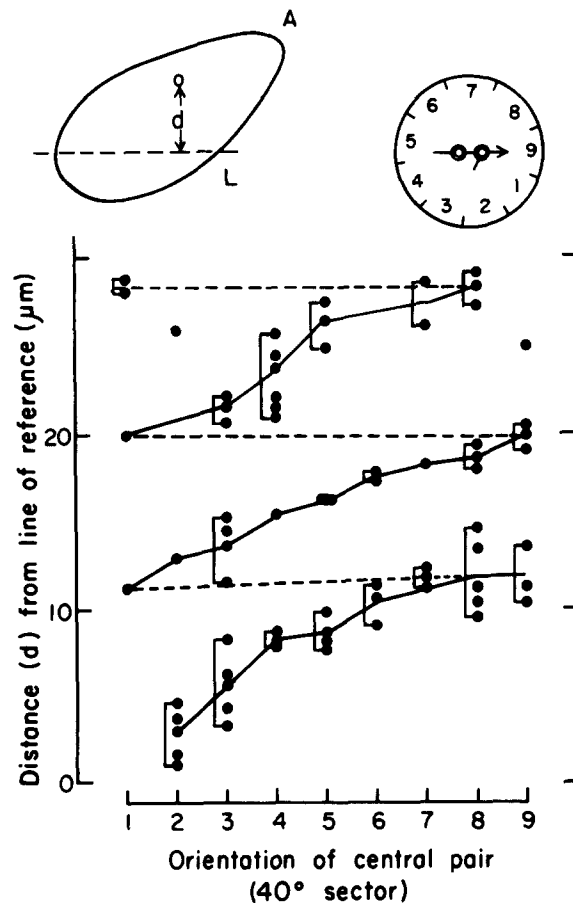


FIGURE 6 The relation of central-pair orientation (ordinate) and the distance from a line of reference (abscissa) in a paramecium instantaneously fixed during backward swimming. Each point indicates a cilium. The central-pair orientation is classified into nine  $40^\circ$  sectors. Sector 9 is defined as the orientation when the vector drawn from the central tubule without to the one with the ultrastructural markers is in the direction of the effective stroke. This stroke is "reversed" i.e., shifted  $120^\circ\text{--}150^\circ$ , in backward-swimming cells. The direction of the effective stroke always parallels the line of synchrony (Fig. 1). The remaining eight sectors are numbered clockwise (seen from the tip of the cilium), as diagrammed. The line of reference is from the paramecium's posterior right to anterior (A) left (L) as marked by the dotted line in the sketch of the cell. This line of reference is a line *B* from the computerized covariance analysis, best fitting the clusters of cilia with the same central-pair orientation (see text). This line approximates the line of synchrony and the direction of the effective stroke. Note that as the distance to the line of reference (*d*) decreases there is a gradual shift in the central-pair orientation in the counterclockwise direction. This pattern has been previously found in cells instantaneously fixed during forward swimming (29, 30), although the effective-stroke direction is very different. Three complete shifts of the orientation are found within the  $30\text{-}\mu\text{m}$  distance examined in this cell. The distance for one complete shift is comparable to the metachronal wavelength as estimated by independent methods (see text).

waves [29]). A plot of the central-pair vector angle vs. distance from this line is shown in Fig. 7*a*. There is clearly no systematic change in the central-pair angle. Furthermore, no systematic changes of the central-pair orientation can be found when other arbitrarily chosen lines of reference are used.

The "sluggish" mutants (23) swim about very slowly and are most often stopped at the bottom of the culture vessel. Their cilia lack clear metachronal waves. Scanning electron micro-

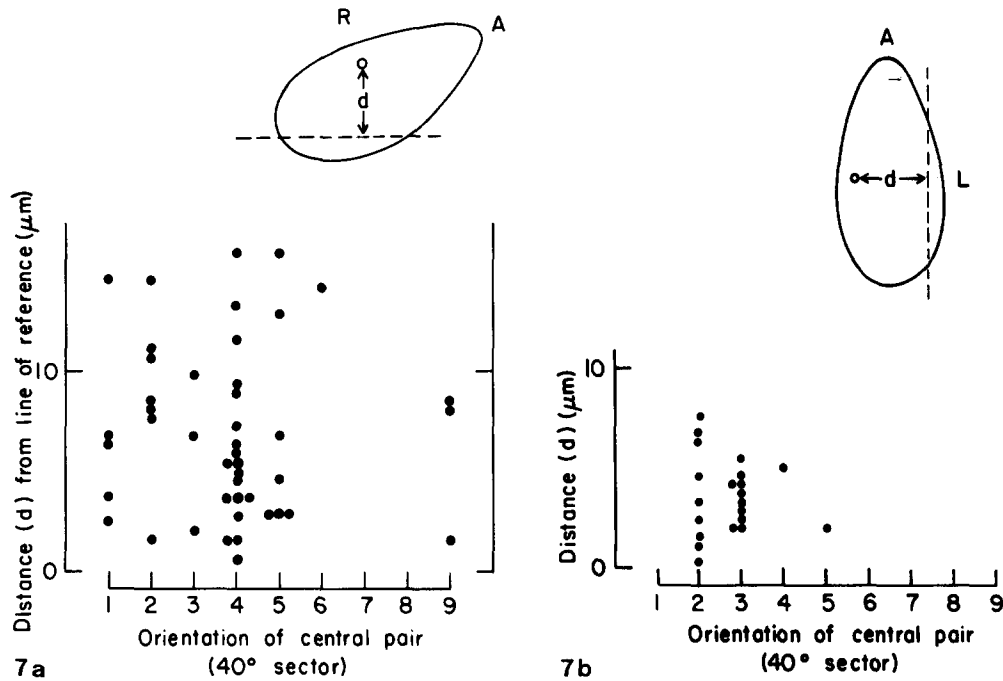


FIGURE 7 (a) The relation of the central-pair orientation (ordinate) and the distance from a line of reference (abscissa) for a cell fixed instantaneously after nickel immobilization. Each point indicates a cilium. Central-pair orientation is defined as number 9 when pointing towards the anterior (arbitrarily chosen because no lines of synchrony are found on these cells) and numbered clockwise (as seen from the tip). The line of reference is a line of best fit (line *B*) from a mock analysis as described in the text. Note that no systematic change of the orientation of the central tubules can be found. (b) The relation of central-pair orientation (ordinate) plotted against the distance from the line of reference (abscissa) for sluggish mutant fixed instantaneously. Each point indicates a cilium. Vector orientation is defined as number 9 pointing towards the anterior (arbitrarily chosen because no lines of synchrony are found in these cells) and numbered clockwise (as seen from the tip). The line of reference comes from a mock analysis as described in the text. Note that the central-tubule orientation is clustered in two adjacent sectors, reflecting the more synchronous pattern of the cilia in this mutant.

graphs of these mutants fixed instantaneously seem to indicate that the cilia are more synchronous than metachronous in beating pattern.

The map of central-pair orientation shows that the central-pair vector angles are almost exclusively in two adjacent sectors. A mock analysis gave a line of best fit parallel to the long axis of the cell, reflecting the oblong shape of the central portion of the paramecium examined. The plot using this line as reference is shown in Fig. 7*b*. Again, it is clear that no systematic change in the central-pair vector angle occurs.

In both the  $\text{Ni}^{++}$ -paralyzed cells and the sluggish mutants, the lack of active beat and, therefore, the loss of the metachronal waves corresponds to the lack of systematic shifts of central-pair orientation. These observations further support the view that central-pair rotation is related to active beat of the cilia.

### Serial Thin Section of Individual Cilia

If the force that causes the rotation is not evenly distributed along the length of the cilium, the central pair will not be expected to be straight, but twisted along its length. Individual cilia are therefore examined for the configuration of their central-pair microtubules. Several types of cilia were chosen for this analysis, all from actively swimming cells fixed instantaneously.

Although the insertion into the axosome cannot be used as a marker at more distal regions, the 10-nm spur can be seen throughout the length of the cilium. A vector can be drawn from the central tubule without to the one with the spur at any

height along the cilium. The angle between this vector and an arbitrary line of reference changes from distal to proximal sections of individual cilia. This indicates twists of the central pairs. Because the precision in angle measurements of the central-pair vector is estimated at  $<10^\circ$ , any significant change must be  $\geq 10^\circ$ . The change in the vector angles between any two consecutive thin sections in a series is expected and found to be small. Thus, several sections in a series are needed to determine whether the central pairs are indeed twisted.

Fig. 8 shows the data from two cilia in two consecutive grids of serial sections with an unknown number of sections lost between grids. Both cilia exhibit clear and progressive changes in the angle of their central-tubule vector. This angle shifts  $>100^\circ$  between the two extreme sections. Because the more distal sections have larger angles, both cilia have central pairs that form left-handed helices. Although the quantitation is imprecise, Fig. 8 suggests that the central pair along the same cilium can be twisted to different degrees at different regions. Qualitative observations of over 100 cilia in serial sections indicate a twist of the central pair. Central-pair angles from 29 segments of 27 cilia were measured in this manner and the results are summarized in Table I. The first four entries to Table I are the four distal segments from the two cilia shown in Fig. 8. Serial sections of cilia located along a line of synchrony (i.e., cilia in a similar phase of beat), but through segments of widely different heights up the cilia were sampled in cilia 5–20. Although the amount of twist through the eight sections varies from  $3^\circ$  (cilium 16) to  $58^\circ$  (cilium 13), all the twists are left-handed. The last nine cilia in Table I have their

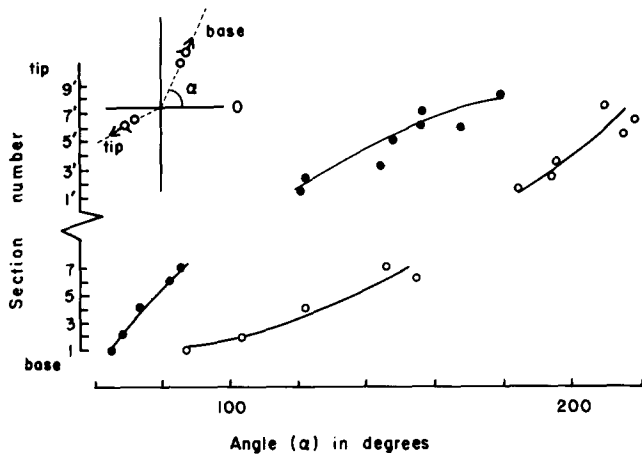


FIGURE 8 Changes of the orientation of the central pairs along the length of two cilia. Central-pair orientation in degrees (from an arbitrary line of reference) is plotted against the number of thin sections in series for two cilia (O and ●). The data are derived from serial sections on two grids (section 1-7 from grid 1 and section 1'-9' from grid 2 with an unknown number of sections lost between the two grids). The angles are measured from the line of reference to the central-pair vector looking from the base as shown in the inset. A change over  $100^\circ$  in the orientation is seen between the two extreme sections in each cilium. The larger angles toward the tip of the cilia indicate left-handed twists of the central pair in these cilia.

central-pair vectors at nine different sections (as defined above). Presumably, these are cilia in various phases of the beat. The change in the central-pair vector angles in the proximal segments were measured. These cilia also show a left-handed twist in their central pair. Thus, all cilia examined show left-handed twists in their central pairs, although in two cases, the twists are not significant.

Except for the first four entries in Table I, which were chosen for their large angular change to demonstrate twist in the central pairs (Fig. 8), the other cilia were not selected with respect to the change in central-pair angles. Cilia 5-20 are all the cilia along one line of synchrony and the last nine cilia were randomly picked among cilia of one cell with their central-pair angles at all possible orientations. Cilia 1-20 were those from backward-swimming cells, cilia 21-29 from a forward-swimming cell. The data collectively indicate that the central pair always forms a left-handed helix, although the pitch of the helix is uneven along the length of the cilium. The average angular change per section is  $3^\circ$ . Using 70 nm as an estimate of averaged section thickness, average angular change is  $43^\circ/\mu\text{m}$  (range  $5^\circ$ - $122^\circ/\mu\text{m}$ ).

### Thick Sections

The left-handed twist of the central-pair microtubules can be more directly demonstrated with high-voltage electron microscope studies of thick (0.25-1.0  $\mu\text{m}$ ) sections.

If two short tubules are aligned exactly parallel to each other, a line of sight parallel to the longitudinal axis of the tubules will allow a clear view through the lumens of both of the tubules. If the two short tubules are not parallel but twisted on each other, two lines of sight at different angles will be needed to give a clear view through the two lumens, one at a time (Fig. 9a). The goniometer stage on the AEI EM 7 HVEM allows  $>60^\circ$  tilt from  $<20^\circ$  to  $>80^\circ$ . With this tilt mechanism and the ability to rotate the stage about the center of the viewing field

TABLE I  
Changes of Central-Pair Orientation along Individual Cilia

| Cilium | Total angular change | No. of sections | Angular change/section |
|--------|----------------------|-----------------|------------------------|
| 1      | +21                  | 7               | +3.4                   |
| 2      | +59                  | 8               | +7.4                   |
| 3      | +60                  | 7               | +8.6                   |
| 4      | +25                  | 8               | +3.1                   |
| 5      | +28                  | 8               | +3.5                   |
| 6      | +26                  | 8               | +3.3                   |
| 7      | +24                  | 8               | +3.0                   |
| 8      | +20                  | 8               | +2.5                   |
| 9      | +13                  | 8               | +1.6                   |
| 10     | +19                  | 8               | +2.4                   |
| 11     | +23                  | 8               | +2.9                   |
| 12     | +35                  | 8               | +4.4                   |
| 13     | +58                  | 8               | +7.3                   |
| 14     | +10                  | 8               | +1.3                   |
| 15     | +29                  | 8               | +3.6                   |
| 16     | +3                   | 8               | +0.4                   |
| 17     | +10                  | 8               | +1.3                   |
| 18     | +34                  | 6               | +5.7                   |
| 19     | +17                  | 8               | +2.1                   |
| 20     | +28                  | 8               | +3.5                   |
| 21     | +25                  | 8               | +3.1                   |
| 22     | +11                  | 7               | +1.6                   |
| 23     | +14                  | 8               | +1.8                   |
| 24     | +8                   | 8               | +1.0                   |
| 25     | +16                  | 12              | +1.3                   |
| 26     | +14                  | 12              | +1.2                   |
| 27     | +28                  | 12              | +2.3                   |
| 28     | +42                  | 15              | +2.8                   |
| 29     | +51                  | 11              | +4.6                   |

Data come from measurements of the central-tubule vector angle (see text and Fig. 6) of segments of cilia serially sectioned. Entries 1-4 are the four distal segments of two cilia shown in Fig. 6. Entries 5-20 are cilia along one line of synchrony but with the analyzed segments at different heights up the cilia. Cilia 21-29 are examined near the base and are at various phases of the beat. "Total angular change" in degrees is the angle difference between the central-tubule vector at the two extreme sections in the series. This total change divided by the number of sections yields the "angular change per section." "+" Means that the distal section is more counterclockwise (looking from the base) than the proximal one. "-" Would have meant the opposite. That there are no "-" data emphasizes the lack of right-handed twist in any of the ciliary segments sampled.

rather than the center of the grid, one can look through at least one of the two central tubules at a time. If in this process, lumens of both central tubules are clearly seen, the central tubules are parallel. If not, from one image alone, we can conclude that the central pair is twisted. To decipher the handedness of the twist, one must obtain two images of the sample taken at different tilt angles of the stage. From a favorably oriented and tilted pair, one can determine the handedness and the amount of a twist. Such twists are indeed found in the thick sections of cilia. The difference between the two tilt angles divided by 2 gives the degree of tilt from the axonemal axis. The pitch of the twist can be estimated by the equation  $2\pi r/\text{degree of tilt}$ . The pitch of the helix of the central pair by such calculation for the region shown in Fig. 9a is  $47^\circ$ .

An even more direct demonstration of the twist in the central pair is by stereo pairs of ciliary cross sections. Fig. 9b and c show such stereo pairs. Because the "thick" sections are only 0.5  $\mu\text{m}$ , the twist is not always evident in the stereo pairs and the degree of twist varies greatly. However, all such stereo pairs ( $n > 30$ ) in which central-pair twists are seen have been found to have left-handed twists. In the case shown in Fig. 9c, the



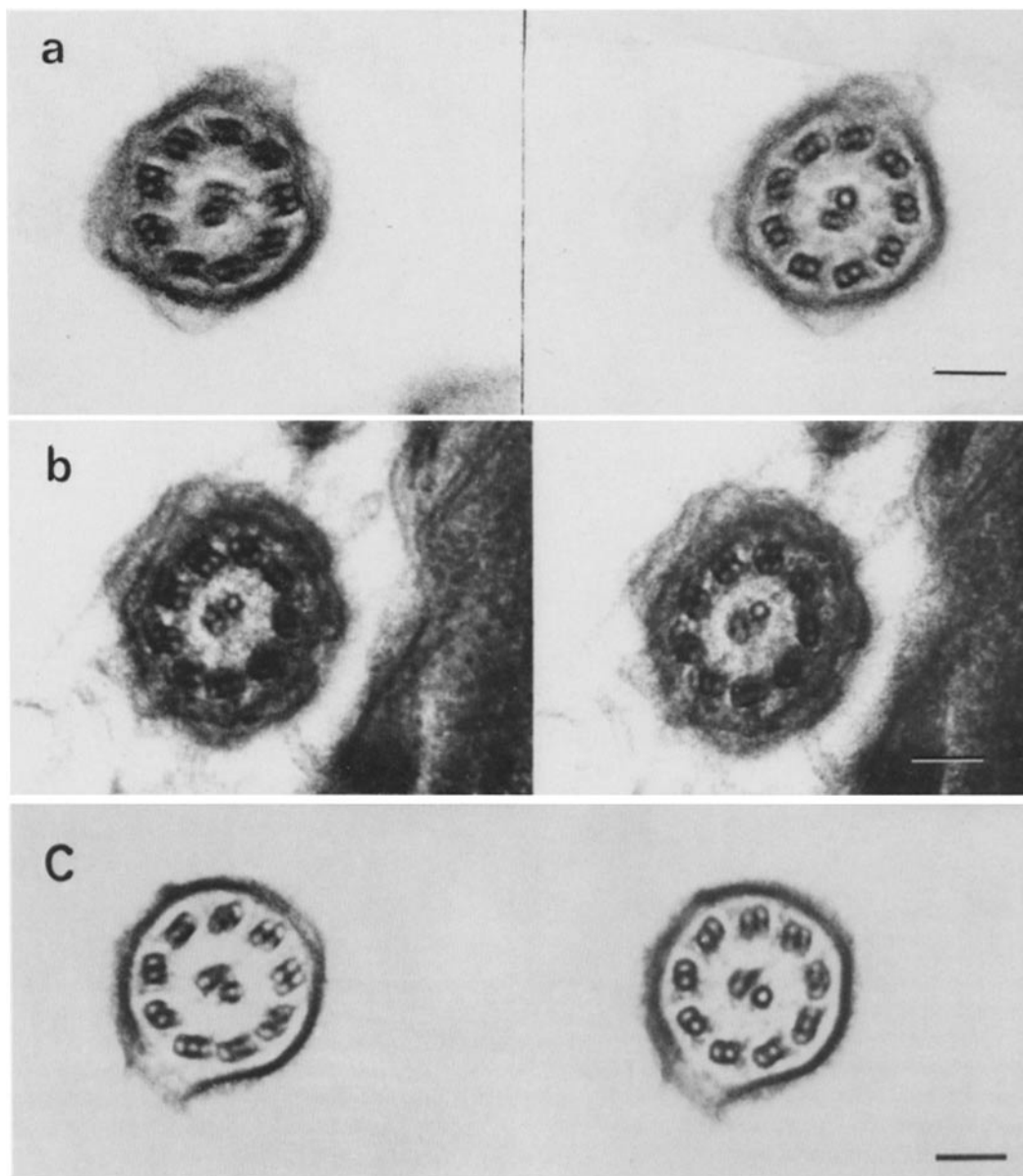


FIGURE 9 Thick sections of cilia. (a) Tilt pairs of a thick section of a cilium from a paramecium viewed under a high-voltage electron microscope. The section is  $0.5 \mu\text{m}$  thick. When the goniometer stage of the microscope is tilted at  $46^\circ$ , the lower member of the central pair is seen through its lumen, while the upper member gives a blurred image (left). When the stage is tilted to  $54^\circ$ , the upper member of the pair is in view straight through its lumen, while the image of the lower member becomes blurred (right). Thus, the axes through the two central tubules are clearly not parallel, but in the form of a twist. (b) A stereo pair of a thick cross section of a paramecium cilium showing a left-handed twist of its central-pair microtubules. This section is  $0.5 \mu\text{m}$  thick and viewed under HVEM. The images are separated by a  $2^\circ$  tilt angle. (c) A stereo pair of a thick cross section of a paramecium cilium showing a left-handed twist of its central-pair microtubules and a right-handed twist of its peripheral-tubule assembly. Bars,  $0.1 \mu\text{m}$ .  $\times 90,000$ .

peripheral-tubule assembly has a right-handed twist, opposite from the twist of the central pair.

### Longitudinal Thin Section

The above analyses indicate that there is a left-handed twist in central pairs. Such a twist should also be evident in longitudinal sections of cilia.

Longitudinal views of cilia showing the central tubules for more than  $1 \mu\text{m}$  are difficult to find in one section, because cilia of this length are seldom in one plane. The amount of information available is greatly increased when two or three sections in a series are studied. By scoring for views 1–3 of

central tubules in longitudinal sections as described in Fig. 5 one can infer the central-pair orientation along the length of the cilium. In a single section or a few serial sections, central-pair orientation with respect to the section plane is seen to change. Fig. 10 is an example showing this change in central-pair angle. The shift from 1 (the view with only one tubule visible) to 3 (the view with both central tubules and space between them visible) indicates that there is a  $90^\circ$  change in the central-pair orientation. (A  $270^\circ$  change is unlikely here.) An accurate determination of the central-pair angle is not possible because the classification of the three views is imprecise. However, a rough estimate indicates that a  $90^\circ$  change in

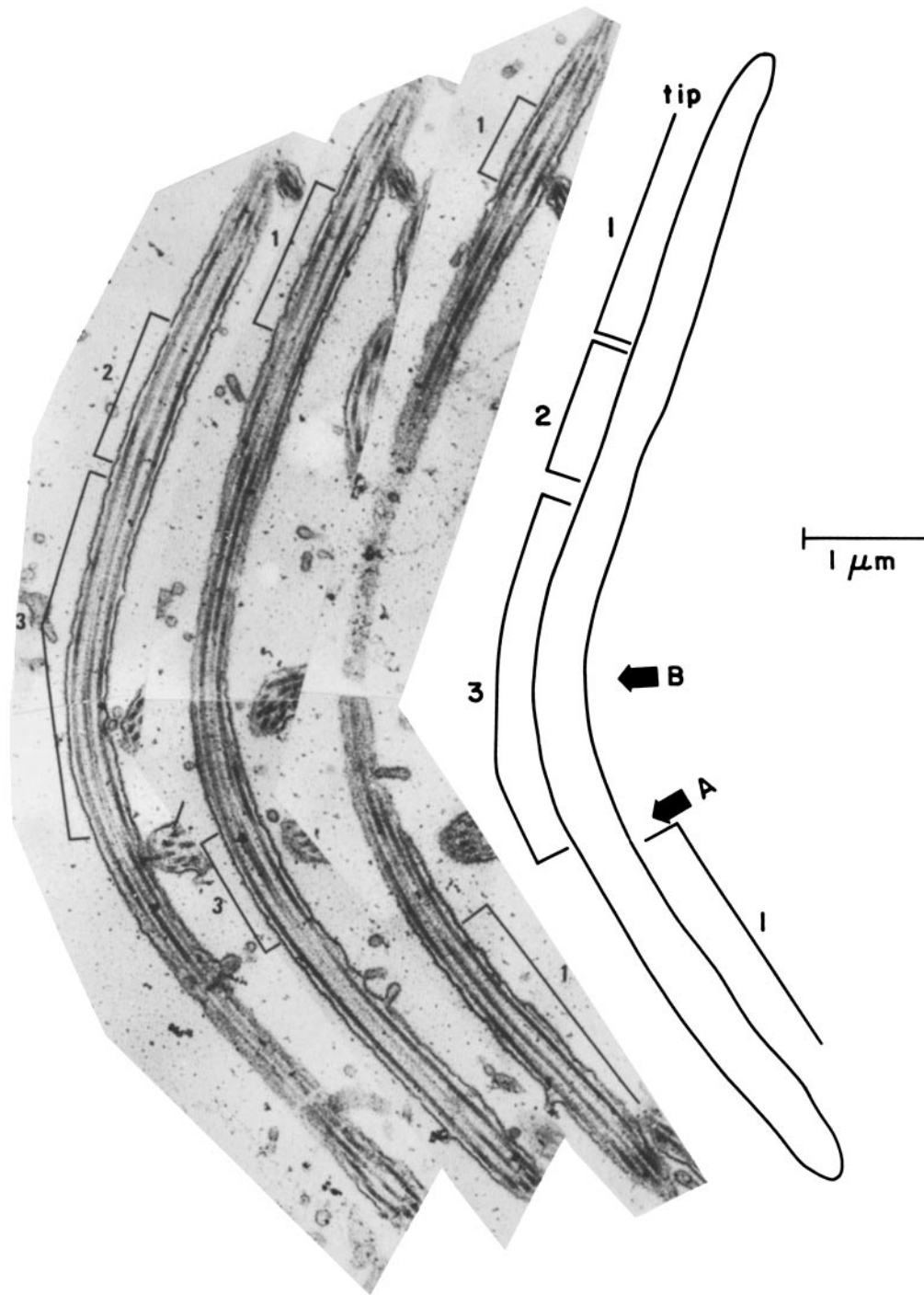


FIGURE 10 Longitudinal sections of a cilium showing changes in the central-pair orientation. The central pair forms three different images (1, 2, and 3), depending on its orientation with respect to the section plane as described in the text and Fig. 3. The classification is only valid when the section covers the central portion of the cilium, as shown by the proper distance between peripheral doublets at opposite sides of the ciliary circumference. When the section misses the central portion of the cilium, images of closely packed peripheral doublets appear near the mid-line of the long section. For a distance of  $>1 \mu\text{m}$ , serial sections are needed to capture the central pair in long view throughout this length. Three serial sections covering a length of  $8 \mu\text{m}$  of the cilium are shown here. The information on the central-pair orientation is compiled in the diagram shown on the right. Note that the central-pair orientation changes from view 1 to view 3 as it enters the bend (point B) from the proximal region (bottom). It changes again through view 2 to view 1 after it leaves the bend in the more distal region (top). The region within the bend has the two central tubules aligned in parallel with the direction of the bend, giving view 3. There appears to be a region (point A) of large change of central-pair orientation just proximal to the bend region. Bar,  $1 \mu\text{m}$ .  $\times 18,000$ .

orientation can be seen within  $1\text{--}2 \mu\text{m}$ . This is the range of the twist-per-distance estimate derived from serial cross-sectional analysis. The change from 1 to 3 or vice versa occurs in a wide

range of distances. The length of the region in which one configuration is continually seen is also variable. This means that the tightness of the twist along the length of the cilium is

uneven. This observation is also consistent with the cross-sectional analysis, where the amount of twist per micrometer ranges from  $5^\circ$  to  $122^\circ$ . The handedness of the twist cannot be determined from the longitudinal thin sections because more than one arrangement of the tubules can give each of the three views (see legend to Fig. 6).

An unexpected finding in such longitudinal sections concerns the orientation of the central pair with respect to the plane of the ciliary bend. We found that in the region of bend, the two central tubules are aligned on a plane which is parallel (14 out of 15), instead of perpendicular, to the direction of the bend. In the case shown in Fig. 10, both the plane through the two central tubules in the region of the bend and the bend direction parallel the section plane. This observation contradicts those by similar analysis of sea urchin sperm (13), where the central pair was found always to be perpendicular to the bend direction. Our finding bears on the argument that the rotation and the twist of the central pair may not be a passive consequence of ciliary motion (see Discussion).

## DISCUSSION

### *Rotation of the Central Pair*

Our analysis of the central-pair angles of cilia on the surface of *Paramecium* indicates that the central pairs rotate. In cells fixed while swimming forward, the central-pair angle changes systematically in the counterclockwise direction. These changes parallel the organization of cilia fixed at subsequent phases of the beat. When the swimming direction is changed and the line of synchrony reoriented, as in backward-swimming cells, the systematic changes in the central-pair angle also reorient. The changes are sequential in the same direction (counterclockwise), as in the forward-swimming cells. In both cases, the distances between groups of cilia with similar central-pair orientation are comparable to the metachronal wavelength estimated independently in more distal sections of the same cells or from scanning electron micrographs of similarly fixed cells. Furthermore, cells lacking metachronal waves caused by  $\text{Ni}^{++}$  treatment or by a mutation do not have systematic changes in the central-pair orientation.

These results lead to the conclusion that the central-pair orientation is related to the ciliary beat cycle. The simplest interpretation of the changes in central-pair orientation is that the central pair orientation is that the central pair rotates  $360^\circ$  with each beat cycle. The rotation is in the same direction in both forward- and backward-swimming cells. This constancy may reflect a similarity in the form of the three-dimensional ciliary beat in both directions.

### *Rotation of the Whole Axoneme?*

The central pair appears to rotate with respect to the peripheral doublets as well as with respect to markers outside the cilium. In our studies, we examined the region just above the basal body. There is no evidence in the literature that the basal body rotates. Salisbury and Floyd (38) have shown that the striated fibers attached to the basal bodies in rhizoplasts of a green algae contract in high concentrations of  $\text{Ca}^{++}$ . However, we have found no statistically significant difference in periodicity in the kinetodesmal fibers between the cells fixed during forward and backward swimming, two forms of locomotion known to correlate with two different physiological concentrations of internal  $\text{Ca}^{++}$  (Nizamuddin and Kung, unpublished observations). Even if the  $\text{Ca}^{++}$  causes the fibers to contract

and the contraction moves the basal body, because  $\text{Ca}^{++}$  concentration does not change during the beat cycle, it is reasonable to assume little or no movement in the basal body during the ciliary beat cycle.

If the axoneme as a whole rotates with respect to the anchored basal body, one would expect a very large twist just above the basal body because this is the region in which we find central-pair rotation. Such a twist of the whole axoneme is not observed in longitudinal thin section or thick sections of our preparation. Transmission electron microscopy of these sections and high-resolution scanning electron microscopy of Triton-treated specimens often show  $\sim 15^\circ$ – $20^\circ/\mu\text{m}$  twists of the whole assembly of the peripheral doublets along the full length of the axoneme. The handedness of these twists is not fixed (29). Thus, in thick sections, the twist of the peripheral-doublet assembly and the twist of the central pair are often of the opposite sense. The opposite sense of the peripheral and the central twists further argues against the rotation of the axoneme as a whole.

### *Twist of the Central Pair*

All three methods of analyzing the configuration of the central pair show that twists indeed exist. Furthermore, whenever the handedness of the central-pair twist can be determined, it is left-handed. This is consistent with the view that the central pair rotates counterclockwise with the rotation being generated at the base.

The number and variety of cilia sampled make it highly unlikely that the central pair ever has a right-handed twist. This means either that the central pair has a static left-handed twist or that a twist is generated by the rotation of the central pair at the base and propagated towards the tip or both.

We found a large range in the degree of twist per unit distance, indicating that the twist is uneven along the length of the cilium. The uneven tightness of the left-handed twist along the cilium may be systematic. Analysis of longitudinal sections, as in Fig. 10, often shows that the twist is tighter just below the ciliary bend. At and distal to the bend, the twist is slight. During the recovery stroke of paramecium cilia, the bend propagates from the base of the cilium towards the tip. This bend propagation may be correlated with the propagation of a region of tight twist just below the bend.

### *Continuous Rotation?*

The simplest interpretation of the various central-pair orientations found across the metachronal waves is that central pair rotates. For example, a  $40^\circ$  counterclockwise rotation is considered more likely than a  $320^\circ$  clockwise rotation in explaining the shift of the central-pair orientation from sector 2 to sector 1 seen in two adjacent cilia. Therefore, the continuous rotation of the central pair in one direction described above is the simplest interpretation of the data, but not the only possible interpretation.

The frequency distribution of central-pair orientation is not even. In both the forward- and backward-swimming paramecia, there are more central pairs oriented toward certain sectors. If this uneven distribution reflects reality, rather than being caused by sampling errors, one may argue for a more complex interpretation of the data. For example, the central pair might rotate counterclockwise for several sectors then quickly rotate clockwise back. This would explain why few or no cilia are caught with their central pair oriented toward certain sectors.

The alternative interpretation consistent with the hypothesis of continuous counterclockwise rotation is that the rotation is not of even speed and the uneven distribution of the central-pair angles simply reflects the uneven distribution of the time spent at various parts of the beat cycle. The paramecium ciliary beat is composed of a fast, planar effective stroke that comprises some  $\frac{1}{3}$  to  $\frac{2}{3}$  of the beat cycle (Fig. 1 and reference 24) and a slow three-dimensional recovery stroke. Viewed from above the paramecium surface, the tip of each cilium traces a semi-circle in each beat cycle, with the recovery stroke along the arc and the effective stroke the chord. If the central-pair rotation reflects this beat asymmetry, one would expect the rotation to be uneven in speed, traversing certain sectors representing the effective stroke much faster than those corresponding to the recovery stroke, i.e., fewer cilia will be caught in the sectors for the effective stroke. Because of the uncertainty in relating the patterns in more distal sections to those at the proximal region where the analysis on central-pair orientation is performed, we cannot at present relate a specific orientation of the central pair to a specific phase of the beat cycle.

Regardless of whether the central pair is actively leading or passively following the rest of the cilium (see below), we can correlate the rotation of the central pair to the beat cycle. Viewed from above, the cilium has a continuous counterclockwise motion. The correlated counterclockwise rotation of the central pair might, therefore, also be expected to be continuous.

We have not encountered a right-handed twist in any study of the configuration of the central pair. Our postulate that the twist is related to ciliary motion is consistent with a left-handed twist being a reflection of the continuous counterclockwise rotation of the central tubule.

An indication of what might be the continuous counterclockwise rotation of the central pair has been given by Jarosch and Fuchs (20). They describe the movement of a stiff fibril projecting out from the tips of the *Synura* flagella. They show that this fibril rotates and the period of its rotation is equal to the time required for a bend on the flagellum to travel one wavelength.

A direct demonstration of central-pair rotation has been made by cinematography of the flagellum of *Micromonas pusilla* (Omoto and Witman, unpublished observations). This flagellum is essentially a long central-tubule pair protruding from a short 9 + 2 stub as described by Manton (25).

### Is the Rotation Active or Passive?

Many references in the literature contend that the central pairs are oriented perpendicular to the plane of the bend (9, 12, 13, 35, 48, 49). Although this is most likely the case during some portion of the effective stroke and perhaps other parts of the beat cycle, our observations indicate that it is not always the case. Fig. 10 clearly shows that the plane through the two central tubules can be parallel to the plane of the bend in *Paramecium* cilia. The contention in the literature is largely derived from cross-sectional analysis. From such, the bend direction and location can only be deduced indirectly. Therefore, the orientation of the central pair with respect to the bend cannot be certain. Our results disagree with the one longitudinal analysis of sea urchin sperm tails (13). The conflicting results might be because of the use of different types of cilia, the use of cilia at different parts of their beat cycles (effective or recovery stroke), different methods of "freezing" cilia (instantaneous fixation or fixing in rigor) or different methods of sample preparation. Holwill et al. (19) have recently re-an-

alyzed the data from tip analysis of Satir (39) and argue that the bend plane, at least in certain regions along the flagellum, is not normal to the surface containing the central pair of microtubules.

In discussions of whether the change in orientation of the central pair is a passive or an active process, it has been pointed out that the state of lowest potential energy for such a pair of tubules occurs when the plane through the two tubules is perpendicular to the bend plane of the cilium (9, 12). Because the central pairs have previously been deduced to be perpendicular to the bend plane, it was then argued that the central pair passively responds to the movement of the rest of the cilium during the beat. Because in our study, the central pair is not perpendicular but parallel to the bend plane for long distances in most of the cilia examined, it can be argued that, at least in certain parts of the beat cycle, the central-pair orientation is not simply a passive process on account of the bend.

Rather than being a passive process, the rotation of the central pair may be an active one, initiated or constantly driven by a mechanism(s) other than bending. To account for the counterclockwise rotation and the left-handed twist of the central pair, this mechanism should be at the proximal end of the central tubules. The region of the cilium where the central tubules terminate is highly specialized (7). The complex structural features in this region could encompass such a mechanism. In this connection, it is interesting to note that Dentler (5) has demonstrated by histochemistry, phosphatase activity in the axosome where the central tubules terminate in *Tetrahymena*. Our preliminary results in *Paramecium* confirm this finding (Schobert and Kung, unpublished observations).

### A Model

Although many dynein-related activities and proteins have been identified (1, 14), data to date indicate that the dynein arms' attachments to different peripheral tubules are chemically and structurally equivalent, except for the apparently permanently attached arms between peripheral doublets 5 and 6 in certain metazoan cilia. If we assume that all dynein arms on peripheral tubules are equivalent, then how can their activities be modulated to produce the ciliary motion? Self-regulation of the arms through a feedback mechanism cannot explain the initiation and the re-initiation of a bend (4, 18). The finding that the central pair is twisted and changes its orientation with respect to the peripheral doublets during the beat cycle in *Paramecium* raises the possibility that the central pair may play an important role in the coordination and regulation of the sliding of different doublets at different regions, and at different times.

On the basis of our and others' observations, we propose a model to describe the mechanism of ciliary motility. For the active sliding between two neighboring doublets to be effective and form a bend, these doublets must be in a certain position with respect to the central tubules. As this position moves toward the tip, the bend propagates. Around the circumference of the axosome, only certain doublets attain this position at any one time. For a strictly planar motion, sequential active sliding of more and more distal regions of one or a few doublets on one quadrant of the cilium may be sufficient. For a three-dimensional motion, all peripheral doublets reach this position and slide actively but at different heights along the cilium at different times. The rotation of a twisted central pair distributes this activity among the nine doublets during the three-dimen-

sional beat of the cilium.

This model specifies that (a) the central pair is a necessary component in the regulatory mechanism of the "9 + 2" axoneme, (b) the orientation of the central pair with respect to the assembly of the peripheral tubules determines the interaction between neighboring peripheral doublets, (c) rotation of the central pair is generated at the base and is at least partly independent of peripheral tubule activity.

These points are briefly discussed below:

(a) Should the regulatory mechanism be sought outside the dynein arms themselves, the central-pair microtubules are the logical candidate. This pair with nonidentical members is usually the only asymmetric structure inside the generally radially symmetric peripheral-tubule assembly and it is strategically located in the center. In species where central tubules are normally present, deletion of the central pair or even a projection of the central pair by mutations results in paralyzed cilia (53) even though dynein arms of these mutants seem to be normal in structure and function. There are, however, specialized flagella and sperm tails that do not possess central tubules, but nevertheless can beat (1, 33). The requirement for special types of motility in these cases may have generated alternative regulatory mechanisms through the course of evolution.

(b) The structural connection between the peripheral doublets and the central pair is the radial spokes. Warner and Satir (51) have shown the interaction between the radial spokes and the central pair. There is a systematic change in the spoke orientation at the bend region. These authors postulate that the spoke-central sheath interaction converts the sliding to bending. Mutant cilia missing radial spokes are paralyzed (32, 45, 53). The nine spoke heads connected to the nine peripheral doublets face the asymmetric central pair and its associated structures differently, and therefore are not expected to interact with the central structures in the same way. If the spoke-sheath interaction is indeed important in allowing the slide or converting the slide to the bend, it is reasonable that the slide only occurs on one side of the axoneme. The position for active sliding referred to in our model is the position where the radial spoke of a particular doublet is so aligned that the interaction between this spoke and a certain facet of the central-pair complex is possible.

Rosenthal and Linck (36) showed that of the nine, only doublet 7, doublet 5 and 6 as one unit, and sometimes doublet 4 in demembrated rat sperm tail can show the sliding disintegration without protease treatments. These authors raise the possibility that flagellar wave propagation is brought about not only by the instantaneous sliding of all nine doublet microtubules, but rather by a mechanism wherein the doublets are sequentially activated and coordinated with the axoneme.

Warner (50) and Zanetti et al. (54) demonstrated a selective release of dynein arms from the adjacent tubules with ATP. In *Tetrahymena* cilia, the doublets are numbered with respect to the central tubules, because no independent criteria for numbering peripheral doublets are available. Therefore, it is not clear whether there is selective release at certain doublets or selective release of any of the nine, depending on the orientation of the central pair. If the central pair rotates in *Tetrahymena* cilia as in *Paramecium* cilia, Warner's observations are consistent with our view that the orientation of the central pair determines which peripheral doublets have functional dynein cross-bridges.

(c) The proximal end of the central tubules have special properties. They have unique structures as demonstrated by

thin-section electron microscopy (7), as well as enzymatic activity shown by EM histochemistry (5). Functional uniqueness of the proximal region has been shown. After laser or shear breaking of flagella, bends can only be generated by proximal segments (15, 16). The interesting exception is in a case where, in intact organism, bend can be initiated from the distal tip. In such a case, distal as well as proximal pieces can beat (17).

We suggest that the central pair and its associated structures, such as the sheath and the spur, may be important in circular coordination, i.e., in determining which of the nine peripheral doublets should slide actively. Combining the longitudinal and the circular restrictions, active sliding probably occurs only between one pair of the doublets near the bend at any given moment during the beat. During the recovery stroke of *paramecium* cilia, the bend propagates distally and more and more counterclockwise in time. Our finding that the central pair is twisted and that the twist appears to be more severe just proximal to the bend suggests the possibility that the distal and counterclockwise propagation of this severe twist is correlated with, and perhaps is a part of the mechanism of, bend propagation.

Our hypothesis does not include an explanation for the differentiation of the beat cycle into the effective and the recovery stroke. There is currently no satisfactory explanation for this differentiation. Nor does the hypothesis deal with the effect of  $Ca^{++}$  on the axoneme. Tamm (48) recently showed that all the ultrastructures including the central-pair orientation remain constant in the comb-plate cilia of the ctenophore *Pleurobrachia*, even when the plates are beating in the reverse direction. Apparently, the increase in internal  $Ca^{++}$  causes a phase reversal such that the original effective-stroke direction is now the recovery-stroke direction. This interesting finding on these cilia with a two-dimensional beat is not unlike our finding on the *Paramecium* cilia with a three-dimensional beat. We found (Fig. 6 and references 29 and 30) that the central pair rotates counterclockwise in both the forward- and the backward-swimming *paramecia*. Thus the  $Ca$ -induced ciliary reversal in both *Pleurobrachia* and *Paramecium* does not seem to change the basic way in which the cilia operate. The  $Ca^{++}$  appears to change the "program" that governs the stroke differentiation. Tamm's finding, however, does emphasize that at two different internal  $Ca^{++}$  concentrations, the same central-pair orientation can be correlated with two recovery strokes in the opposite directions. Binding of  $Ca^{++}$  to the central complex or the spokes may affect the way they interact. This finding also shows the important difference between cilia with two-dimensional and three-dimensional beat.

The core of our hypothesis, namely that the central-pair orientation specifies the sliding of certain peripheral tubules, can explain many of the observations of axonemal behavior and can help to solve the puzzle of the regulation of the peripheral doublet activity.

We are indebted to Dr. H. Ris for his invaluable expertise in obtaining and evaluating high-voltage electron micrographs and for his continued encouragement throughout this study. We are also grateful to the staff of the HVEM facility at Madison, Wis.

This work was supported in part by National Institutes of Health grant GM-22714 and National Science Foundation grant BNS 77-20440.

Received for publication 31 January 1980, and in revised form 27 May 1980.

## REFERENCES

1. Baccetti, B., A. G. Burrini, R. Dallai, and V. Fallini. 1979. The dynein electrophoretic bands in axonemes naturally lacking the inner or the outer arms. *J. Cell Biol.* 80:334-340.
2. Bray, D. F., and E. B. Wagenaar. 1978. A double-staining technique for improved contrast of thin sections from Spurr-embedded tissue. *Can. J. Bot.* 56:129-132.
3. Brokaw, C. J. 1972. Computer simulation of flagellar movement. I. Demonstration of stable bend propagation and bend initiation by sliding filament model. *Biophys. J.* 12: 564-586.
4. Brokaw, C. J., and I. R. Gibbons. 1975. Mechanism of movement in flagella and cilia. In *Swimming and Flying in Nature*. T. Y-T. Wu, C. J. Brokaw, and C. Brennan, editors. Plenum Press, New York. 89-126.
5. Dentler, W. L. 1977. Fine structural localization of phosphatases in cilia and basal bodies of *T. pyriformis*. *Tissue Cell.* 9:209-222.
6. Dryl, S. 1959. Antigenic transformation of *P. aurelia* after homologous anti-serum treatment during autogamy and conjugation. *J. Protozool.* 6:25.
7. Dute, R., and C. Kung. 1978. Ultrastructure of the proximal region of somatic cilia in *P. tetraurelia*. *J. Cell Biol.* 78:451-464.
8. Eckert, R., and P. Brehm. 1979. Ionic mechanism of excitation in *Paramecium*. in *Annual Review of Biophys. and Bioeng.* 8:353-383.
9. Fawcett, D. W., and K. R. Porter. 1954. A study of the fine structure of ciliated epithelia. *J. Morphol.* 94:221-264.
10. Frasca, J. M., and V. R. Parks. 1965. A routine technique for double staining ultrathin sections using uranyl and lead salts. *J. Cell Biol.* 25:157-161.
11. Gibbons, B. H., and I. R. Gibbons. 1976. Functional recombination of dynein I with demembrated sea urchin sperm partially extracted with KCl. *Biochem. Biophys. Res. Commun.* 73:1-6.
12. Gibbons, I. R. 1961. The relationship between the fine structure and direction of beat in gill cilia of a lamellibranch mollusc. *J. Biophys. Biochem. Cytol.* 11:170-205.
13. Gibbons, I. R. 1975. The molecular basis of flagellar motility in sea urchin spermatozoa. In *Molecules and Cell Movement*. S. Inoué and R. E. Stephens, editors. Raven Press, New York. 207-232.
14. Gibbons, I. R., E. Fronk, B. H. Gibbons, and K. Ogawa. 1976. Multiple forms of dynein in sea urchin sperm flagella. In *Cell Motility Book C*. R. Goldman, T. Pollard and J. Rosenbaum, editors. Cold Spring Harbor Laboratory, Cold Spring Harbor, N. Y. 915-932.
15. Goldstein, S. F. 1969. Irradiation of sperm tails by laser microbeam. *J. Exp. Biol.* 51:431-441.
16. Goldstein, S. F. 1979. Behavior of short flagellar fragments. *J. Cell Biol.* 83(2, Pt. 2): 181a (Abstr.).
17. Goldstein, S. F., M. E. J. Holwill, and N. R. Silvester. 1970. The effects of laser microbeam irradiation on the flagellum of *Criethidia* (*Strigomonas oncopeltii*). *J. Exp. Biol.* 53:401-409.
18. Hines, M., and J. J. Blum. 1978. Bend propagation in flagella. I. Derivation of equations of motion and their simulation. *Biophys. J.* 23:41-57.
19. Holwill, M. E. J., H. J. Cohen, and P. Satir. 1979. A sliding microtubule model incorporating axonemal twist and compatible with three-dimensional ciliary bending. *J. Exp. Biol.* 78:265-280.
20. Jarosch, R., and B. Fuchs. 1975. Zur fibrillenrotation in der *Synura-Geissel*. *Protoplasma.* 85:285-290.
21. Jurand, A. and G. G. Selman. 1969. *The Anatomy of Paramecium aurelia*. McMillan, London.
22. Kung, C. 1971. Genic mutants with altered system of excitation in *P. aurelia*. I. Phenotype of the behavioral mutants. *Z. Vgl. Physiol.* 71:142-164.
23. Kung, C., S. Y. Chang, Y. Satou, J. Van Houten and H. Hansma. 1975. Genetic dissection of behavior in *Paramecium*. *Science (Wash. D. C.)* 188:898-904.
24. Machemer, H. 1972. Ciliary activity and the origin of the metachrony in *Paramecium*: Effects of increased viscosity. *J. Exp. Biol.* 57:239-259.
25. Manton, I. 1959. Electron microscopical observations on a very small flagellate: The problem of *Chromulina pusilla*. *J. Mar. Biol. Assoc.* 38:319-333.
26. Morgan, J. L., P. H. Crowley, C. J. Benham, T. L. Hayden, and S. M. Lenhart. 1979. Model for wave generation by eukaryotic flagella. *J. Cell Biol.* 83(2, Pt. 2):177a (Abstr.).
27. Mollenhauer, H. H. 1964. Plastic embedding mixtures for use in electron microscopy. *Stain Technol.* 39:111-114.
28. Nelson, D. L., and C. Kung. 1978. Behavior of *Paramecia*: Chemical, physiological and genetic studies. In *Taxis and Behavior*. G. L. Hazelbauer, editor. Chapman and Hall, London. 75-100.
29. Omoto, C. K. 1979. Microtubule orientation and movement during ciliary motion in *Paramecium*. Thesis. University of Wisconsin, Madison, Wis.
30. Omoto, C. K., and C. Kung. 1979. The pair of central tubules rotates during ciliary beat in *Paramecium*. *Nature (Lond.)* 279:532-534.
31. Parducz, B. 1967. Ciliary movement and coordination in ciliates. *Int. Rev. Cytol.* 21:91-128.
32. Piperno, G., B. Huang, and D. J. L. Luck. 1977. Two-dimensional analysis of flagellar proteins from wild-type and paralyzed mutants of *Chlamydomonas reinhardtii*. *Proc. Natl. Acad. Sci. U. S. A.* 74:1600-1604.
33. Prensier, G., E. Viver, S. Goldstein, and J. Schrenel. 1980. Motile flagellum with a "3 + 0" ultrastructure. *Science (Wash. D. C.)* 207:1493-1494.
34. Reynolds, E. S. 1963. The use of lead citrate at high pH as an electron-opaque stain in electron microscopy. *J. Cell Biol.* 17:208-212.
35. Ringo, D. L. 1967. Flagellar motion and fine structure of the flagellar apparatus in *Chlamydomonas*. *J. Cell Biol.* 35:543-571.
36. Rosenthal, E. T., and R. W. Linck. 1979. Sequential regulation of doublet microtubule sliding in demembrated rat sperm models. *J. Cell Biol.* 83(2, Pt. 2):181a (Abstr.).
37. Sale, W. S., and P. Satir. 1977. Direction of active sliding of microtubules in *Tetrahymena* cilia. *Proc. Natl. Acad. Sci. U. S. A.* 74:2045-2049.
38. Salisbury, J. L., and G. L. Floyd. 1978. Calcium-induced contraction of the rhizoplast of a quadriflagellate green alga. *Science (Wash. D. C.)* 202:975-977.
39. Satir, P. 1968. Studies on cilia. III. Further studies on the cilium tip and a "sliding filament" model of ciliary motility. *J. Cell Biol.* 39:77-94.
40. Satir, P. 1974. The present status of sliding microtubule model of ciliary motion. In *Cilia and Flagella*. M. A. Sleight, editor. Academic Press, Inc., New York. 131-142.
41. Shinyogi, C., A. Murakami, and K. Takahashi. 1977. Local reactivation of Triton-extracted flagella by iontophoretic application of ATP. *Nature (Lond.)* 265:269-270.
42. Sonneborn, T. M. 1970. Methods in *Paramecium* research. *Methods Cell Physiol.* 4:241-339.
43. Sonneborn, T. M. 1975. Species designation and description of the 14 syngens of *Paramecium aurelia*. *Trans. Am. Microsc. Soc.* 94:155-178.
44. Spurr, A. R. 1969. A low-viscosity epoxy resin embedding media for electron microscopy. *J. Ultrastruct. Res.* 26:31-43.
45. Sturgess, J. M. 1978. Human cilia defective in radial spokes—a congenital anomaly associated with disease of the respiratory tract. *J. Cell Biol.* 79(2, Pt. 2):298a (Abstr.).
46. Summers, K. E., and I. R. Gibbons. 1971. Adenosine triphosphate-induced sliding of tubules in trypsin-treated flagella of sea urchin sperm. *Proc. Natl. Acad. Sci. U. S. A.* 68: 3092-3096.
47. Summers, K. E., and I. R. Gibbons. 1973. Effects of trypsin digestion of flagellar structures and their relationship to motility. *J. Cell Biol.* 58:618-629.
48. Tamm, S. L. 1979. Ionic and structural basis of ciliary reversal in ctenophores. *J. Cell Biol.* 83(2, Pt. 2):174a (Abstr.).
49. Tamm, S. L., and G. A. Horridge. 1970. The relation between the orientation of the central fibrils and the direction of beat in cilia of *Opalina*. *Proc. Roy. Soc. London Ser. B.* 175: 219-233.
50. Warner, F. D. 1978. Cation-induced attachment of ciliary dynein crossbridges. *J. Cell Biol.* 77:R19-R26.
51. Warner, F. D., and P. Satir. 1974. The structural basis of ciliary bend formation. Radial spoke positional changes accompanying microtubule sliding. *J. Cell Biol.* 63:35-63.
52. Witman, G. B., R. Fay, and J. Plummer. 1976. *Chlamydomonas* mutants: Evidence for the roles of specific axonemal components in flagellar movement. In *Cell Motility Book C*. R. Goldman, T. Pollard, and J. Rosenbaum, editors. Cold Spring Harbor Press. Cold Spring Harbor, New York. 969-986.
53. Witman, G. B., J. Plummer, and G. Sander. 1978. *Chlamydomonas* flagellar mutants lacking radial spokes and central tubules. Structure, composition and function of specific axonemal components. *J. Cell Biol.* 76:729-747.
54. Zanetti, N. C., D. R. Mitchell, and F. D. Warner. 1979. Effects of divalent cations on dynein cross-bridging and ciliary microtubule sliding. *J. Cell Biol.* 80:573-588.